# Roles of Histidines 154 and 189 and Aspartate 139 in the Active Site of Serine Acetyltransferase from *Haemophilus influenzae*[†]

Rong Guan,[‡] Steven L. Roderick,[§] Bin Huang,[§] and Paul F. Cook*,[‡]

*Department of Chemistry and Biochemistry, University of Oklahoma, 620 Parrington Oval, Norman, Oklahoma 73019, and Department of Biochemistry, Albert Einstein College of Medicine, Yeshiva University, 1300 Morris Park Avenue, Bronx, New York 1046*

*Received January 15, 2008; Revised Manuscript Received April 9, 2008*

ABSTRACT: A crystal structure of serine acetyltransferase (SAT) with cysteine bound in the serine subsite of the active site shows that both H154 and H189 are within hydrogen-bonding distance to the cysteine thiol [Olsen, L. R., Huang, B., Vetting, M. W., and Roderick, S. L. (2004) *Biochemistry 43*, 6013−6019]. In addition, H154 is in an apparent dyad linkage with D139. The structure suggests that H154 is the most likely catalytic general base and that H189 and D139 may also play important roles during the catalytic reaction. Site-directed mutagenesis was performed to mutate each of these three residues to Asn, one at a time. The $V_1/E_t$ value of all of the single mutant enzymes decreased, with the largest decrease (~1240-fold) exhibited by the H154N mutant enzyme. Mutation of both histidines, H154N/H189N, gave a $V_1/E_t$ ~23700-fold lower than that of the wild-type enzyme. An increase in $K_{Ser}$ was observed for the H189N, D139N, and H154N/H189N mutant enzymes, while the H154N mutant enzyme gave an 8-fold decrease in $K_{Ser}$. For all three single mutant enzymes, $V_1/E_t$ and $V_1/K_{Ser}E_t$ decrease at low pH and give a p$K_a$ of about 7, while the $V_1/E_t$ of the double mutant enzyme was pH independent. The solvent deuterium kinetic isotope effects on $V_1$ and $V_1/K_{Ser}$ decreased compared to wild type for the H154N mutant enzyme and increased for the H189N mutant enzyme but was about the same as that of wild type for D139N and H154N/H189N. Data suggest that H154, H189, and D139 play different catalytic roles for SAT. H154 likely serves as a general base, accepting a proton from the $\beta$-hydroxyl of serine as the tetrahedral intermediate is formed upon nucleophilic attack on the thioester carbonyl of acetyl-CoA. However, activity is not completely lost upon elimination of H154, and thus, H189 may be able to serve as a backup general base at a lower efficiency compared to H154; it also aids in binding and orienting the serine substrate. Aspartate 139, in dyad linkage with H154, likely facilitates catalysis by increasing the basicity of H154.

Serine acetyltransferase (SAT)[1] catalyzes the conversion of acetyl-CoA and L-serine to CoA and *O*-acetyl-L-serine (OAS), the first and rate-limiting step of the biosynthesis of L-cysteine in bacteria and higher plants (*1, 2*).

SAT is a member of the hexapeptide repeat acyltransferase superfamily, which has imperfect tandem repeats of a hexapeptide sequence described as [LIV]-[GAED]-$X_2$-[STAV]-X (*3, 4*). The repeat sequences generate an unusual left-handed parallel $\beta$-helix (L$\beta$H) domain (*5*) that generates an equilateral prism-like structure. All of the enzymes are trimeric (SAT is a dimer of trimers) with the L$\beta$H domains forming a triangular structure. The active site is found at the interface between two L$\beta$H domains.

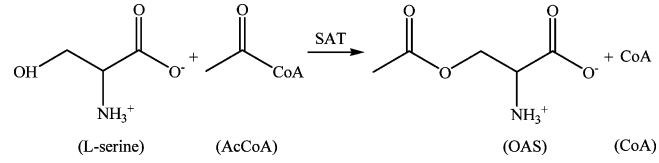


A sequential kinetic mechanism was proposed for serine acetyltransferase from *Haemophilus influenzae* (*Hi*SAT) with AcCoA bound first, followed by L-serine, and with release of OAS prior to CoA (*6*). On the basis of the pH dependence of kinetic parameters and solvent isotope effects, a chemical mechanism has been proposed (Figure 1) (*7*). The reaction begins with nucleophilic attack of the $\beta$-hydroxyl of serine on the thioester carbonyl of acetyl-CoA catalyzed by a general base to give a tetrahedral intermediate. The general base then functions as a general acid, donating a proton to the sulfur atom of CoA, once the tetrahedral intermediate has collapsed to give the products, OAS and CoA.

The crystal structure of *Hi*SAT with cysteine bound at the L-serine subsite of the active site shows H154 and H189 within hydrogen-bonding distance to the cysteine thiol; H154 is in dyad linkage to D139 (Figure 2) (*8*). The SAT exhibits

[†] This work is supported by the Grayce B. Kerr Endowment to the University of Oklahoma (to P.F.C.).

* Corresponding author. E-mail: pcook@ou.edu. Tel: 405-325-4581. Fax: 405-325-7182.

[‡] University of Oklahoma.

[§] Albert Einstein College of Medicine.

[1] Abbreviations: AcCoA, acetyl-coenzyme A; CoA, coenzyme A; OAS, *O*-acetyl-L-serine; OASS, *O*-acetylserine sulfhydrylase; *Hi*SAT, serine acetyltransferase from *Haemophilus influenzae*; L$\beta$H, left-handed parallel $\beta$-helix; DTNB, 5,5′-dithiobis(2-nitrobenzoate); BSA, bovine serum albumin; TNB, 5-thio-2-nitrobenzoate; Mes, 2-(*N*-morpholino)-ethanesulfonic acid; Ches, 2-(*N*-cyclohexylamino)ethanesulfonic acid; Tris, tris(hydroxymethyl)aminomethane; Hepes, *N*-(2-hydroxyethyl)piperazine-*N*′-2-ethanesulfonic acid; $D_2O$, deuterium oxide; SKIE, solvent deuterium kinetic isotope effect; IPTG, isopropyl $\beta$-D-1-thiogalactopyranoside.

10.1021/bi800075c CCC: $40.75 
Published on Web 05/23/2008

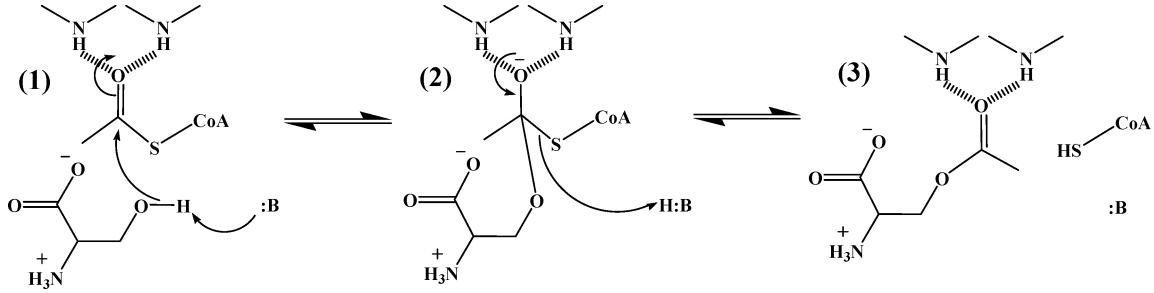


FIGURE 1: Proposed chemical mechanism of *Hi*SAT. (1) E−AcCoA−serine complex. (2) Tetrahedral intermediate. (3) E−CoA−OAS complex.

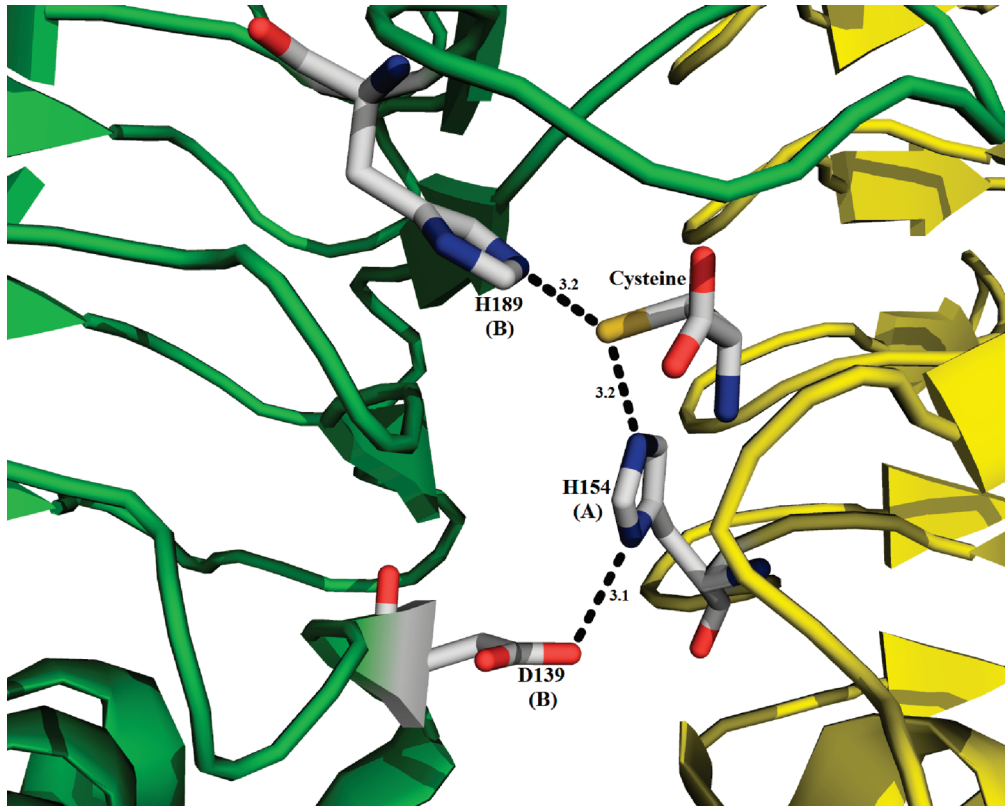


FIGURE 2: Close-up of the active site of *Hi*SAT with cysteine bound. Locations of two subunits of the trimer of *Hi*SAT are shown in yellow and green, respectively. The dashed lines represent potential hydrogen bonds, and the numbers close to dashed lines are distances in Å. The (A) and (B) next to numbered residues indicate the subunit that contributes the residue. The figure was created using Pymol from DeLano Scientific LLC. The *Hi*SAT structure with cysteine bound has an access number of 1SSQ in the Protein Data Bank.

mechanistic similarities to other L$\beta$H enzymes which have a His-Asp (Glu) catalytic dyad (*9*). Amino acid sequence alignments of 15 SATs (*10*) indicate complete conservation of H154 and H189, while D139 can be either Asp or Glu.

In this paper, the roles of H154, H189, and D139 were investigated. Site-directed mutagenesis was used to make three single mutant enzymes by changing these three residues to Asn, one at a time, and a double mutant enzyme, changing H154 and H189 to Asn at the same time. Initial velocity studies, pH−rate profiles, and solvent deuterium kinetic isotope effects were carried out to characterize the mutant enzymes. Data are discussed in terms of the overall mechanism of SAT.

## MATERIALS AND METHODS

*Chemicals.* L-Serine, DTNB, and AcCoA were from Sigma. The buffers Mes, Tris, Hepes, and Ches were from Research Organics, Inc. Deuterium oxide (99.9 atom % D) was from Cambridge Isotope Laboratories, Inc. All other chemicals and reagents were obtained from commercial sources, were of reagent grade, and were used without purification.

*Plasmid Construction and Site-Directed Mutagenesis.* The *cysE* gene encoding *Hi*SAT (GenBank accession number P43886) was cloned into a pET28a vector via the *Nde*I/*Bam*HI sites (*8*). Site-directed mutagenesis was performed using the QuikChange method to make three single mutant enzymes by changing H154, H189, and D139 to Asn, one at a time, and a double mutant, H154N/H189N, by mutating H189 to Asn in the H154N mutant enzyme. The templates for the single and double mutant enzymes were the recombinant *Hi*SAT plasmid and the mutated H154N plasmid, respectively. The oligonucleotide primers to generate the mutations are listed in Table 1. The resulting mutant genes were sequenced at the Laboratory for Genomics and Bioinformatics of the University of Oklahoma Health Science Center to be certain that no mutations other than

Table 1: Sequence of Oligonucleotide Primers[a]

| | |
|---|---|
| $H154N_f$ | GGCCACGGAATTATGTTCGAC**AAT**GCAACAGGTATTGTTGTGG |
| $H154N_r$ | CCACAACAATACCTGTTGC**ATT**GTCGAACATAATTCCGTGGCC |
| $H189N_f$[b] | CGGGAAAAGAATCAGGCGATCGT**AAT**CCCAAAGTACGCGAGGGTG |
| $H189N_r$[b] | CACCCTCGCGTACTTTGGG**ATT**ACGATCGCCTGATTCTTTTCCCG |
| $D139N_f$ | CAGTAGCTTTCGATGTA**AAT**ATTCACCCAGCGGCG |
| $D139N_r$ | CGCCGCTGGGTGAAT**ATT**TACATCGAAAGCTACTG |

[a] Codons for mutation are in bold. Subscripts f and r represent forward and reverse primers, respectively. [b] These two primers were used to make the H154N/H189N double mutant, and the plasmid of H154 was the template.

the one desired were present; none were found. All constructs encoded an N-terminal 6-His-tagged enzyme. Plasmids were transformed into *Escherichia coli* BL21-(DE3)-RIL cells for expression.

*Enzyme.* The strain containing the mutated plasmid was grown overnight at 37 °C in 50 mL of LB medium with 30 $\mu$g/mL kanamycin. This culture was transferred into 1 L of LB/kanamycin medium on the morning of the next day, and the cell growth was continued at 30 °C until the $A_{600}$ reached 0.7. IPTG was added to a final concentration of 1 mM to initiate expression. After 4 h of induction at 30 °C, the cells were harvested by centrifugation at 4500*g* for 30 min. The cell pellet was suspended in 50 mM phosphate, 300 mM NaCl, and 10 mM imidazole, pH 8.0, and sonicated on ice for 3 min with a 30 s pulse followed by a 1 min rest, using a MISONIX Sonicator XL. The supernatant was obtained by centrifugation at 20000*g* for 30 min and then loaded onto a Ni-NTA column with a 6 mL bed volume. The column was washed with 6 volumes of 20 mM imidazole at pH 8.0, and enzyme was eluted with 3 volumes of 250 mM imidazole, pH 8.0. The purified enzyme was then dialyzed against 20 mM Tris, 50 mM NaCl, and 10% glycerol at pH 7.5 and stored frozen at −80 °C. The wild-type and mutant enzymes, with the exception of D139N, were purified in the same way. For D139N, 10% glycerol was added to sonication, wash, and elution buffers, and the dialysis buffer was 20 mM Tris, 600 mM NaCl, and 50% glycerol at pH 7.5.

*Enzyme Assays.* In the forward reaction direction, the appearance of CoA was coupled to the production of TNB via a disulfide exchange reaction with DTNB (*11*). Initial rates were calculated using an extinction coefficient of 14150 $M^{-1}$ $cm^{-1}$ for TNB at 412 nm (*12*). Reactions were carried out at room temperature in 1 cm path length cuvettes in a final volume of 0.3 mL. Reaction mixtures contained 100 mM buffer, 0.45 mM DTNB, variable amounts of AcCoA and L-serine, and an appropriate amount of enzyme. Reaction was initiated by addition of enzyme. A unit of enzyme is defined as the amount of enzyme required to produce 1 $\mu$mol of product in 1 min at 25 °C. The wild-type *Hi*SAT was stabilized by adding 100 $\mu$g/mL BSA when diluted for use in assays (*6*). Rates were measured using a Beckman DU 640 spectrophotometer to monitor the change in absorbance at 412 nm.

*pH Studies.* The initial velocity was measured as a function of AcCoA concentration (0.5−5 $K_m$) at different fixed concentrations of serine (0.5−5 $K_m$). These experiments were carried out as a function of pH to determine the kinetic parameters $V_1$, $V_1/K_{Ser}$, and $V_1/K_{AcCoA}$. The pH was maintained using the following buffers at a concentration of 100 mM in the forward reaction direction: Mes, pH 5.5−6.5; Hepes, pH 6.5−8.5; Ches, pH 8.5−10.0. The pH was measured before and after the reaction with observed changes smaller than 0.1 pH unit.

*Solvent Deuterium Kinetic Isotope Effects.* Initial velocity studies were carried out as discussed above in $H_2O$ and $D_2O$ at the pH(D)-independent region of the $V_1$, $V_1/K_{Ser}$, and $V_1/K_{AcCoA}$ pH(D)−rate profiles. The solvent deuterium kinetic isotope effect (SKIE) was then estimated as the ratio of the pH- and pD-independent values of the parameters. The SKIEs were then more accurately obtained by direct comparison of initial rates at a single pH(D) in the pH-independent region of the curve.

*Data Processing.* Data were fitted to appropriate rate equations using the Marquardt−Levenberg algorithm (*13*) supplied with the EnzFitter program or the programs developed by Cleland (*14*). All of the initial rate data were fitted using eqs 1 and 2, which conform to sequential and equilibrium ordered kinetic mechanisms, respectively. Data for pH−rate profiles that decrease with a limiting slope of 1 at low pH were fitted using eq 3, while those that decreased with limiting slopes of 1 and −1 were fitted using eq 4. The SKIE data were fitted using eq 5, which allows the SKIEs on $V$ and $V/K$ to be equal to one another.

$$v = \frac{VAB}{K_{ia}K_b + K_aB + K_bA + AB} \quad (1)$$

$$v = \frac{VAB}{K_{ia}K_b + K_bA + AB} \quad (2)$$

$$\log y = \log\left(\frac{C}{1 + \frac{H}{K_1}}\right) \quad (3)$$

$$\log y = \log\left(\frac{C}{1 + \frac{H}{K_1} + \frac{K_2}{H}}\right) \quad (4)$$

$$v = \frac{VA}{(K_a + A)(1 + F_iE_v)} \quad (5)$$

In eqs 1, 2, and 5, $v$ and $V$ represent initial and maximum velocities, respectively, $A$ and $B$ represent substrate concentrations, $K_a$ and $K_b$ are $K_m$ values for substrates A and B, respectively, and $K_{ia}$ is the dissociation constant for E−AcCoA. In eq 5, $F_i$ is the fraction of $D_2O$ in the solvent, and $E_v$ is the isotope effect minus 1 when the isotope effects on $V$ and $V/K$ are the same. In eqs 3 and 4, $y$ is the value of $V$ or $V/K$ at any pH, while $C$ is the pH-independent value of $y$, $H$ is the hydrogen ion concentration, and $K_1$ and $K_2$ are the acid dissociation constants of functional groups on enzyme or substrate.

## RESULTS

*Kinetic Parameters of the Mutant Enzymes.* Initial velocity patterns were obtained by measuring the initial rates at pH 7.3 using variable concentrations of AcCoA and L-serine;

Table 2: Kinetic Parameters for *Hi*SAT Wild-Type and Mutant Enzymes at pH 7.3

| | $V_1/E_t$ ($s^{-1}$) | $V_1/K_{Ser}E_t$ ($M^{-1}$ $s^{-1}$) | $V_1/K_{AcCoA}E_t$ ($M^{-1}$ $s^{-1}$) | $K_{AcCoA}$ (mM) | $K_{Ser}$ (mM) |
|---|---|---|---|---|---|
| wild type[a] | $360 \pm 10$[b] | $(7.53 \pm 0.07) \times 10^4$ | $(5.1 \pm 0.8) \times 10^5$ | $0.7 \pm 0.1$ | $4.7 \pm 0.4$ |
| H154N | $0.29 \pm 0.02$ | $470 \pm 80$ | $1300 \pm 400$ | $0.21 \pm 0.08$ | $0.6 \pm 0.1$ |
| (fold change) | $-(1240 \pm 90)$[c] | $-(160 \pm 30)$ | $-(390 \pm 140)$ | $-(3 \pm 1)$ | $-(8 \pm 1)$ |
| H189N | $18.7 \pm 0.9$ | $590 \pm 70$ | N/A[d] | N/A | $32 \pm 4$ |
| (fold change) | $-(19 \pm 1)$ | $-(130 \pm 20)$ | | | $+(7 \pm 1)$ |
| D139N | $34 \pm 1$ | $200 \pm 10$ | $(2.7 \pm 0.4) \times 10^5$ | $0.12 \pm 0.02$ | $160 \pm 10$ |
| (fold change) | $-(10.6 \pm 0.4)$ | $-(380 \pm 20)$ | $-(1.9 \pm 0.4)$ | $-(6 \pm 1)$ | $+(34 \pm 4)$ |
| H154N/H189N | $0.0152 \pm 0.0004$ | $0.57 \pm 0.03$ | $64 \pm 3$ | $0.24 \pm 0.02$ | $27 \pm 2$ |
| (fold change) | $-(23700 \pm 900)$ | $-(132000 \pm 7000)$ | $-(8000 \pm 1000)$ | $-(2.9 \pm 0.5)$ | $+(5.7 \pm 0.6)$ |

[a] From Johnson et al. (*6*). [b] Values are ±SE. [c] The symbols, − and +, represent decrease and increase, respectively. [d] N/A is not applicable; $K_{AcCoA}$ is zero in an equilibrium kinetic mechanism.

data are summarized in Table 2. $V_1/E_t$ decreased by about 1240-, 19-, 11-, and 23700-fold for H154N, H189N, D139N, and H154N/H189N, respectively, compared to wild type. The value of $K_{AcCoA}$ decreased for the H154N, D139N, and the H154N/H189N mutant enzymes compared to wild type, while $K_{Ser}$ decreased about 8-fold for H154N but increased by about 7-, 34-, and 6-fold for the H189N, D139N, and H154N/H189N mutant enzymes, respectively. The largest decrease in $V_1/E_t$ among three single mutant enzymes is observed for H154N, suggesting it is important for catalysis, while H189 and D139 are likely important for both binding and catalysis.

*pH Dependence of Kinetic Parameters.* The pH dependence of the kinetic parameters of the mutant enzymes was obtained by measuring initial velocity patterns as a function of pH. All of the mutant enzymes are stable over the pH range studied; the H154N/H189N mutant enzyme is inactive below pH 6.9. In the forward reaction direction, initial velocity studies indicate the kinetic mechanism of the H154N, H189N, and H154N/H189N mutant enzymes is ordered over the entire pH range studied, similar to wild type (*6*), but is equilibrium ordered for H154N below pH 6.3 and for H189N below pH 7.3. However, the kinetic mechanism of the D139N mutant enzyme is random with respect to binding AcCoA and serine, as suggested by the noncompetitive inhibition pattern for glycine vs AcCoA and ATP vs serine; glycine is uncompetitive versus AcCoA for the wild-type enzyme.

$V_1/E_t$ and $V_1/K_{Ser}E_t$ decrease at low pH for all of the single mutant enzymes, giving a limiting slope of 1. A bell-shaped pH−rate profile with limiting slopes of 1 and −1 was obtained for $V_1/K_{AcCoA}E_t$ for D139. $V_1/E_t$ and $V_1/K_{AcCoA}E_t$ are pH independent over the pH range studied for H154N/H189N double mutant enzyme, while $V_1/K_{Ser}E_t$ decreases at low pH with a limiting slope of 1. In the case of the H154N and H189N mutant enzymes, data for the $V_1/K_{AcCoA}E_t$ pH−rate profile could not be collected at low pH, since $K_{AcCoA}$ is zero. $pK_a$ values are summarized in Table 3. pH−rate profiles are plotted in Figure 3 for the H154N, H189N, and H154N/H189N mutant enzymes and in Figure 4 for the D139N mutant enzyme.

*Solvent Deuterium Kinetic Isotope Effects.* Measurement of the $V_1$ and $V_1/K_{Ser}$ in $H_2O$ and $D_2O$ gave about equal values of $^{D_2O}V_1$ and $^{D_2O}(V_1/K_{Ser})$. Values are about the same as those of wild type for D139N and H154N/H189N, slightly lower than wild type for the H154N mutant enzyme, and significantly higher for the H189N mutant enzyme (Table 4). The pH(D) dependence of kinetic parameters was measured over the pH(D) range of 7.3−8.5 to determine the solvent deuterium kinetic isotope effects on $V_1/K_{AcCoA}$ for D139N (Figure 4). An average value about 3.5 was estimated for $^{D_2O}(V_1/K_{AcCoA})$ of D139N.

Table 3: Summary of $pK_a$ Values for Wild-Type and Mutant *Hi*SAT

| | $pK_a \pm$ SE | | |
|---|---|---|---|
| enzyme | $V_1$ | $V_1/K_{Ser}$ | $V_1/K_{AcCoA}$ |
| wild type[a] | $6.8 \pm 0.2$ | $7.2 \pm 0.2$ | N/A |
| H154N | $6.7 \pm 0.2$ | $7.4 \pm 0.4$ | N/A |
| H189N | $7.5 \pm 0.2$ | $8.0 \pm 0.3$ | N/A |
| D139N | $6.2 \pm 0.4$ | $6.1 \pm 0.5$ | $7.2 \pm 0.3$<br>$8.1 \pm 0.2$ |
| H154N/H189N | N/A | $7.8 \pm 0.1$ | N/A |

[a] From Johnson et al. (*7*).

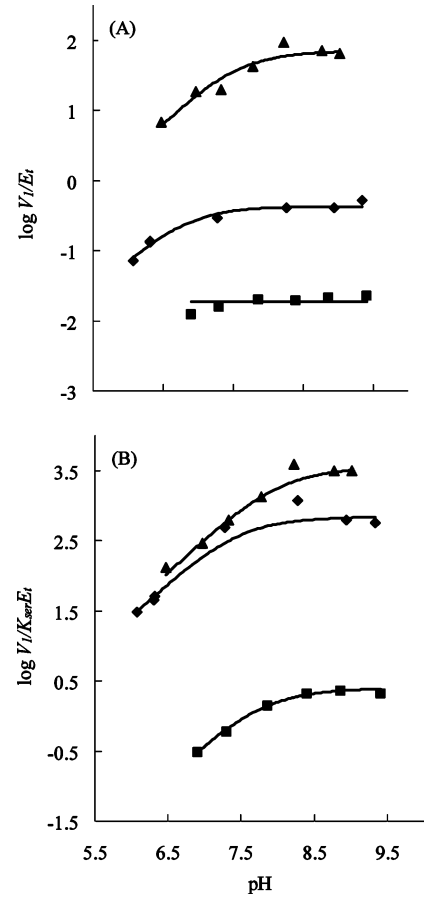


FIGURE 3: pH dependence of $V_1/E_t$ (A) and $V_1/K_{Ser}E_t$ (B) for the H154N, H189N, and H154N/H189N mutant enzymes. Points for the H154N (◆), H189N (▲), and H154N/H189N (■) mutant enzymes are experimental values, while the curves are theoretical, based on fits of the data using eq 3.

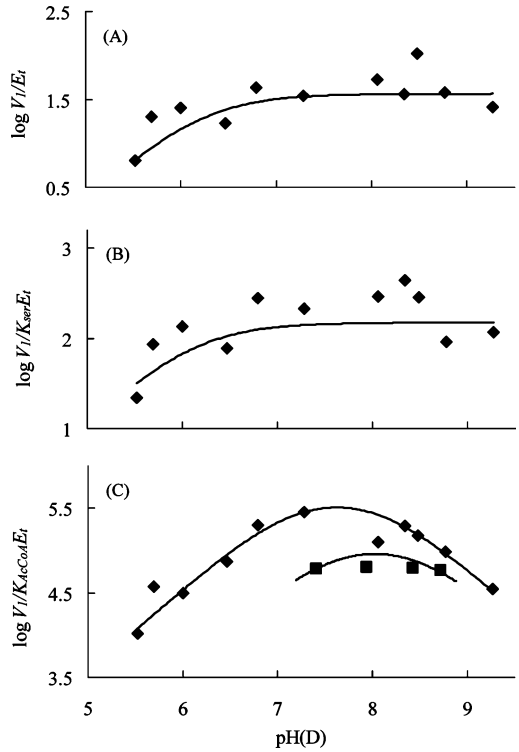


FIGURE 4: pH(D) dependence of $V_l/E_t$ (A), $V_l/K_{Ser}E_t$ (B), and $V_l/K_{AcCoA}E_t$ (C) for the D139N mutant of *Hi*SAT. The points shown are the experimentally determined values. pH and pD dependences are presented by (▲) and (■), respectively. The curves are theoretical, based on fits of the data using eq 3 for the pH−rate profile of $V_l/E_t$ and eq 4 for the pH−rate profile of $V_l/K_{AcCoA}E_t$. The curve for the pD dependence of $V_l/K_{AcCoA}E_t$ and the pH dependence of $V_l/K_{Ser}E_t$ were drawn by hand.

Table 4: Summary of SKIE Values for Wild-Type and Mutant Enzymes

| enzyme | $^{D_2O}V_l$ | $^{D_2O}(V_l/K_{Ser})$ | $^{D_2O}(V_l/K_{AcCoA})$ |
|---|---|---|---|
| wild type [a] | 1.9 ± 0.1 | 2.5 ± 0.4 | N/A |
| H154N | 1.64 ± 0.03 | 1.64 ± 0.03 | N/A |
| H189N | 3.4 ± 0.3 | 3.4 ± 0.3 | N/A |
| D139N | 2.3 ± 0.1 | 2.3 ± 0.1 | 3.5[b] |
| H154N/H189N | 2.2 ± 0.1 | 2.2 ± 0.1 | N/A |

[a] From Johnson et al. (*7*). [b] Estimated graphically as the ratio of the pH(D)-independent values in Figure 4.

## DISCUSSION

*H154N Mutant Enzyme.* Site-directed mutagenesis was used to change H154 to Asn, which cannot act as a general base but can still form a hydrogen bond with D139. The ~1240-fold decrease in $V_l/E_t$ and ~160-fold decrease in $V_l/K_{Ser}E_t$ indicate that H154 is important to catalysis and suggest that it acts as a general base that accepts a proton from the $\beta$-hydroxyl of serine. This result was anticipated given the hydrogen bond distance between H154 and D139, suggesting the two residues might act as a catalytic dyad.

The rate-limiting step for wild-type *Hi*SAT is the formation of the tetrahedral intermediate once the E−AcCoA−serine complex is formed (*7*). In this step, a nucleophilic attack occurs on the carbonyl of the AcCoA thioester by the hydroxyl group of serine, with the general base accepting a proton from the hydroxyl group (Figure 1). The difference in the values of $^{D_2O}V_l$ (~1.9) and $^{D_2O}(V_l/K_{Ser})$ (~2.5) suggested that the chemical step is not the only rate-limiting step for the overall reaction and that release of CoA also contributes to rate limitation, with the rate of product release ~1.5 times faster than that of the chemical step (*7*).

In the case of the H154N mutant enzyme, $^{D_2O}V_l \approx {}^{D_2O}(V_l/K_{Ser}) \approx 1.6$. Since the release of CoA was only 1.5-fold greater than the chemical step(s), the 1240-fold decrease observed for the H154N mutant enzyme is a lower limit and is closer to 1860-fold when correcting for the small contribution made by product release. Therefore, the observed SKIEs are likely intrinsic values. However, the values are lower than those observed for wild type. Considering that the elimination of H154 gives an enzyme that still has H189 in position to potentially act as a base, accepting a proton from the serine hydroxyl, we believe the isotope of 1.6 reflects general base catalysis by H189.

The pH dependence of kinetic parameters provides information on functional groups required on enzyme and/or reactant in a given protonation state for optimum binding and/or catalysis (*15*). The *V*/*K* for a reactant is obtained at a limiting concentration of one reactant and saturating concentrations of all others and reflects the free form of the enzyme that substrate binds to, and the free reactant. *V* is obtained at saturating concentrations of all substrates and reflects the enzyme form(s) that is (are) present in the steady state.

The $V_l/E_t$ and $V_l/K_{Ser}E_t$ of the H154N mutant enzyme decrease at low pH, giving a limiting slope of 1, and exhibit p*K*s of about 6.7 and 7.4, respectively, which are, within error, equal to the p*K*s observed for the wild-type enzyme. These data indicate that the group that acts as a base in the mutant enzyme has a p*K* very similar to that of the wild type. As suggested above, H189 may act as the general base in place of H154 in the mutant enzyme, and the p*K* of 6.7−7.4 would thus reflect this group.

*H189N Mutant Enzyme.* In the case of the H189N mutant enzyme, the mutation eliminates the possibility of H189 acting as a general base. However, the 19-fold decrease in $V_l/E_t$ shows that H189 is important but not essential to catalysis. The 130-fold decrease in $V_l/K_{Ser}E_t$ and 7-fold increase on $K_{Ser}$ indicate that H189 also contributes to the binding of serine. Thus the function of H189 may be that of orienting serine for efficient catalysis.

The observed values of ~3.4 for $^{D_2O}V_l$ and $^{D_2O}(V_l/K_{Ser})$ indicate that chemistry limits the overall reaction. The larger isotope effects suggest that when H154 acts as the base, it is not optimally positioned compared to H189 in the H154N mutant enzyme.[2] The pH−rate profiles for H189N also exhibit a limiting slope of 1 at low pH for $V_l/E_t$ and $V_l/K_{Ser}E_t$. However, the p$K_a$ values have increased to ~7.5 for $V_l/E_t$ and ~8.0 for $V_l/K_{Ser}E_t$, compared to 6.8 and 7.2 obtained for wild type. The increases in the p$K_a$ may result from removal of H189, which is likely protonated in the wild-type enzyme.

*H154N/H189N Mutant Enzyme.* The double mutant enzyme has eliminated H154 and H189 of *Hi*SAT, so that

[2] Recent evidence from the Klinman laboratory (personal communication) suggests hydrogen transfer reactions originate almost solely from quantum mechanical tunneling coupled to the breathing modes (thermal motions) of the protein. Thus, the more compressed the reaction coordinate, the smaller the isotope effect. Thus, H189N with a SKIE of ~3.4 suggests H154 is not optimally placed to act as the catalyst in the proton extraction reaction, while H154N, where H189 is the catalyst, with an SKIE of ~1.6 is better positioned.

neither is able to act as a general base. The activity of the double mutant enzyme is 23700-fold lower, while $V_1/K_{Ser}E_t$ is 132000-fold lower than wild-type values. The decrease in $V_1/E_t$ is the product of the decreases observed for the H154N and H189N mutant enzymes. The $>10^4$-fold decrease is consistent with elimination of general base catalysis in *Hi*SAT. In addition, the $>10^5$-fold lower value of $V_1/K_{Ser}E_t$ likely reflects the $\sim10^4$-fold loss in catalytic function and an ~10-fold loss in affinity for serine. The $V_1/E_t$ value of the H154N/H189N mutant enzyme is 19-fold lower than the value of H154N, which suggests H189 is responsible for most of the activity observed for the H154N mutant enzyme. The increase in $K_{Ser}$ observed for the double mutant enzyme is similar to the change observed for H189N, consistent with the proposed role of H189 in serine binding.

Also consistent with the proposed roles of H154 and H189 is the pH dependence of kinetic parameters. $V_1/E_t$ is pH independent over the pH range 7.5−9.5 and only appears to decrease at low pH (<7.0), where the enzyme is no longer stable. Elimination of both imidazoles thus results in loss of the p$K_a$ for the catalytic group. A p$K_a$ of about 7.8 is observed in the $V_1/K_{Ser}E_t$ profile, but this likely reflects the protonation state of a group that must be protonated for optimum binding of serine in the double mutant enzyme.[3] This may be the same group observed in the $V_1/K_{AcCoA}E_t$ pH−rate profile of the D139N mutant enzyme.

A value of ~2.2 is observed for $^{D}V_1$ and $^{D}(V_1/K_{Ser})$ for the double mutant enzyme, and this is almost certainly an intrinsic effect. However, since it is not known whether catalysis is by water or some other base, it is not possible to further interpret this effect at this point.

*D139N Mutant Enzyme.* Changing D139 to N changes the nature of the putative dyad linkage between D139 and H154 from a strong hydrogen bond between the negatively charged aspartate and $N^{\delta}$ of H154 to a weaker bond to the amide carbonyl oxygen of the asparagine. The mutation results in an 11-fold decrease in $V_1/E_t$, likely a result of decreasing the basicity of H154, a possible general base catalyst. The biggest effect of the mutation is seen as a 34-fold increase in $K_{Ser}$, resulting in a 380-fold decrease in $V_1/K_{Ser}E_t$. The majority of the increase in $K_{Ser}$ is likely associated with a decreased affinity. The decreased affinity may be a reflection of the weaker dyad linkage causing a repositioning of H154, but this will have to await additional studies.

Since H154 is available to act as the general base in the D139N mutant enzyme, and given the large decrease in $V_1/K_{Ser}E_t$, one would expect $^{D_2O}(V_1/K_{Ser})$ to approach a value of ~3.4, which is close to the observed value of $^{D_2O}(V_1/K_{AcCoA})$. However, $^{D_2O}V_1$ and $^{D_2O}(V_1/K_{Ser})$ are smaller with values of ~2.3.

Finite SKIE values on all three kinetic parameters indicate the kinetic mechanism has become random for this mutant enzyme, but it exhibits a steady-state mechanism with binding AcCoA before serine preferred. The relative off-rate of serine and AcCoA from E−AcCoA−serine can be estimated from the isotope effect data and mechanism 6.

[3] An alternative interpretation of the pH−rate profile would be selective binding of the correctly protonated forms of the enzyme and substrate, such that when the enzyme−substrate complex is formed, the protonation state of the enzyme and substrate functional groups are locked. Given the elimination of two active site residues, it is difficult to reconcile this as a reasonable possibility.

On the basis of the mechanism 6, expressions for $V_1$, $V_1/K_{AcCoA}$, and $V_1/K_{Ser}$ and the respective SKIEs are given in eqs 7−9.


(6)

$$V=\frac{k_5k_9}{k_5+k_9} \qquad {}^{D_2O}V=\frac{{}^{D_2O}k_5+\dfrac{k_5}{k_9}}{1+\dfrac{k_5}{k_9}} \tag{7}$$

$$V/K_{Ser}=\frac{k_3k_5}{k_4+k_5} \qquad {}^{D_2O}(V/K_{Ser})=\frac{{}^{D_2O}k_5+\dfrac{k_5}{k_4}}{1+\dfrac{k_5}{k_4}} \tag{8}$$

$$V/K_{AcCoA}=\frac{k_3'k_5}{k_4'+k_5} \qquad {}^{D_2O}(V/K_{AcCoA})=\frac{{}^{D_2O}k_5+\dfrac{k_5}{k_4'}}{1+\dfrac{k_5}{k_4'}} \tag{9}$$

Using the value of $^{D_2O}(V_1/K_{AcCoA})$ (3.5) for $^{D_2O}k_5$ and the value of $^{D_2O}V_1 = {}^{D_2O}(V_1/K_{Ser}) \approx 2.3$, values of $k_5/k_9$ and $k_5/k_4$ are approximately 0.9 and the value of $k_5/k_4'$ is very close to zero. The ratio of $k_5/k_4$ and $k_5/k_4'$ gives a value of $k_4'/k_4$ (the off-rate constant for AcCoA and serine) that would be a very large number. The change in mechanism is consistent with an increase in the off-rate constant for AcCoA from the E−serine−AcCoA complex. Since $V_1/E_t$ was decreased by an order of magnitude, and the pathway with serine adding to E−AcCoA gives isotope effects that are very similar to those of the wild-type enzyme, data suggest a decrease in the rate of all of the steps from addition of serine to release of OAS in mechanism 6. This could result from a decrease in the amount of catalytically active enzyme generated when serine binds, that is nonproductive binding of serine. The large isotope effect observed on $V_1/K_{AcCoA}$ is consistent with an increase in the off-rate constant for AcCoA from the E−serine−AcCoA complex resulting in rate-limiting chemistry. The increased off-rate for AcCoA may result from an inability of AcCoA to generate the catalytically active enzyme as a result of its binding modes as D139 is changed. These two effects may be linked in that enzyme binding of AcCoA to give E−AcCoA may result in a decreased amount of productive enzyme as serine binds. In addition, when serine is bound to give E−AcCoA−serine, AcCoA is released rapidly to give E−serine. It thus appears that D139 in dyad linkage to H154 contributes to generating the catalytically competent E−AcCoA−serine complex.

$V_1/E_t$ and $V_1/K_{ser}E_t$ pH−rate profiles give a limiting slope of 1 at low pH for the D139N mutant enzyme, similar to wild type. However, a bell-shaped pH−rate profile is observed for $V_1/K_{AcCoA}E_t$, with limiting slopes of 1 and −1. The predominant enzyme forms for $V_1/K_{Ser}$ and $V_1/K_{AcCoA}$ in this case are the E−AcCoA and E−serine complexes, respectively, while for $V_1$, the E−AcCoA−serine and E−CoA complexes are likely present. The p$K_a$s observed in

$V_1$ and $V_1/K_{Ser}$ are about 6.2 and 6.1, respectively, about a pH unit lower than that observed for wild type, consistent with a decreased basicity of H154 when D139 is changed to N. The p$K_a$ on the acid side of the $V_1/K_{AcCoA}E_t$ pH−rate profile is ~7.2, a pH unit higher than that observed in $V_1/K_{Ser}E_t$, consistent with formation of a hydrogen bond between H154 and the serine $\beta$-hydroxyl, as expected with H154 acting as a base to accept the proton. The group with a p$K_a$ of ~8.1 shown on the basic side of the $V_1/K_{AcCoA}E_t$ profile was not observed for the wild-type enzyme and is likely important for binding AcCoA since it is not observed in the $V_1/E_t$ pH−rate profile. This group may reflect the protonation state of H189 or some other active site residue.

*Proposed Roles of H154, H189, and D139 in HiSAT.* The kinetic parameters, pH−rate profiles, and SKIEs discussed above provide a picture of how the three catalytic residues might function in the active site of the *Hi*SAT. Optimum binding of reactants requires the dyad composed of H154 and D139. Since these residues are donated to the active site by different subunits at the interface (Figure 2), it is not surprising in retrospect that the catalytic conformation depends on a functional H154-D139 dyad.

Once AcCoA and serine are bound, we propose that $N^{\epsilon}$ of H154 is hydrogen-bonded to the $\beta$-hydroxyl of serine in preparation for accepting a proton as the tetrahedral intermediate between serine and AcCoA is formed. In the ternary complex H189 is likely protonated and donates a hydrogen bond to the serine hydroxyl to properly orient it in the site.

It should be stated at this point that it is possible neither H154 nor H189 serves as a base, and some other enzyme side chain serves in this capacity. However, on the basis of all of the data obtained, we believe this is only a remote possibility.

Interestingly, when H154 is mutated, H189 can serve as an alternative catalyst. The lower activity of H154N compared to wild type suggests there is likely no biological significance to this backup behavior. A similar backup system was reported for fructose 2,6-bisphosphatase (*16*). H256 acts as the nucleophilic catalyst for this enzyme and becomes phosphorylated by fructose 2,6-bisphosphate. A second imidazole side chain (H390) facilitates phosphoryl transfer and acts as a general base catalyst to activate water as the phosphoimidazole is hydrolyzed. Mutation of H256 to Ala gives an enzyme that retains 17% activity. In the H256A mutant enzyme, H390 acts as a general base to directly catalyze the hydrolysis of the 2-phosphate of the fructose 2,6-$P_2$.

## REFERENCES


1. Kredich, N. M., and Tomkins, G. M. (1966) The enzymic synthesis of L-cysteine in *Escherichia coli* and *Salmonella typhimurium*. *J. Biol. Chem. 241*, 4955–4965.
2. Smith, I. K., and Thompson, J. F. (1971) Purification and characterization of L-serine transacetylase and *O*-acetyl-L-serine sulfhydrylase from kidney bean seedlings (*Phaseolus vulgaris*). *Biochim. Biophys. Acta 227*, 288–295.
3. Vaara, M. (1992) Eight bacterial proteins, including UDP-*N*-acetylglucosamine acyltransferase (LpxA) and three other transferases of *Escherichia coli*, consist of a six-residue periodicity theme. *FEMS Microbiol. Lett. 76*, 249–254.
4. Bairoch, A. (1993) The PROSITE dictionary of sites and patterns in proteins, its current status. *Nucleic Acids Res. 21*, 3097–3103.
5. Raetz, C. R., and Roderick, S. L. (1995) A left-handed parallel beta helix in the structure of UDP-*N*-acetylglucosamine acyltransferase. *Science 270*, 997–1000.
6. Johnson, C. M., Huang, B., Roderick, S. L., and Cook, P. F. (2004) Kinetic mechanism of the serine acetyltransferase from *Haemophilus influenzae*. *Arch. Biochem. Biophys. 429*, 115–122.
7. Johnson, C. M., Huang, B., Roderick, S. L., and Cook, P. F. (2004) Chemical mechanism of the serine acetyltransferase from *Haemophilus influenzae*. *Biochemistry 43*, 15534–15539.
8. Olsen, L. R., Huang, B., Vetting, M. W., and Roderick, S. L. (2004) Structure of serine acetyltransferase in complexes with CoA and its cysteine feedback inhibitor. *Biochemistry 43*, 6013–6019.
9. Johnson, C. M., Roderick, S. L., and Cook, P. F. (2005) The serine acetyltransferase reaction: acetyl transfer from an acylpantothenyl donor to an alcohol. *Arch. Biochem. Biophys. 433*, 85–95.
10. Gorman, J., and Shapiro, L. (2004) Structure of serine acetyltransferase from *Haemophilus influenzae* Rd. *Acta Crystallogr. D 60*, 1600–1605.
11. Cook, P. F., and Wedding, R. T. (1978) Cysteine synthetase from *Salmonella typhimurium* LT-2. Aggregation, kinetic behavior, and effect of modifiers. *J. Biol. Chem. 253*, 7874–7879.
12. Riddles, P. W., Blakeley, R. L., and Zerner, B. (1983) Reassessment of Ellman's reagent. *Methods Enzymol. 91*, 49–60.
13. Marquardt, D. W. (1963) An algorithm for least-squares estimation of nonlinear parameters. *J. Soc. Indust. Appl. Math. 11*, 431–441.
14. Cleland, W. W. (1979) Statistical analysis of enzyme kinetic data. *Methods Enzymol. 63*, 103–138.
15. Cleland, W. W. (1977) Determining the chemical mechanisms of enzyme-catalyzed reactions by kinetic studies. *Adv. Enzymol. Relat. Areas Mol. Biol. 45*, 273–387.
16. Mizuguchi, H., Cook, P. F., Tai, C.-H., Hasemann, C. A., and Uyeda, K. (1999) Reaction mechanism of fructose-2, 6-bisphosphatase. A mutation of nucleophilic catalyst, histidine 256, induces an alteration in the reaction pathway. *J. Biol. Chem. 274*, 2166–2175.


BI800075C